Drebrin Autoantibodies in Patients with Seizures and Suspected Encephalitis

Julika Pitsch, PhD,[1] Delara Kamalizade, MPharm,[1] Anna Braun, MS,[1] Julia C. Kuehn, MS,[1]
Polina E. Gulakova, PhD,[1] Theodor Rüber, MD,[2,3] Gert Lubec, MD,[4] Dirk Dietrich, MD,[5]
Randi von Wrede, MD,[2,3] Christoph Helmstaedter, MD,[2,3] Rainer Surges, MD,[2,3]
Christian E. Elger, MD,[2,3] Elke Hattingen, MD,[6] Hartmut Vatter, MD,[5]
Susanne Schoch, PhD,[1,2] and Albert J. Becker, MD [1]

Objective: Assess occurrence of the dendritic spine scaffolding protein Drebrin as a pathophysiologically relevant auto-antibody target in patients with recurrent seizures and suspected encephalitis as leading symptoms.
Methods: Sera of 4 patients with adult onset epilepsy and suspected encephalitis of unresolved etiology and equivalent results in autoantibody screening were subjected to epitope identification. We combined a wide array of approaches, ranging from immunoblotting, immunoprecipitation, mass spectrometry, subcellular binding pattern analyses in primary neuronal cultures, and immunohistochemistry in brains of wild-type and Drebrin knockout mice to in vitro analyses of impaired synapse formation, morphology, and aberrant neuronal excitability by antibody exposure.
Results: In the serum of a patient with adult onset epilepsy and suspected encephalitis, a strong signal at ~70kDa was detected by immunoblotting, for which mass spectrometry revealed Drebrin as the putative antigen. Three other patients whose sera also showed strong immunoreactivity around 70kDa on Western blotting were also anti-Drebrin-positive. Seizures, memory impairment, and increased protein content in cerebrospinal fluid occurred in anti-Drebrin-seropositive patients. Alterations in cerebral magnetic resonance imaging comprised amygdalohippocampal T2-signal increase and hippocampal sclerosis. Diagnostic biopsy revealed T-lymphocytic encephalitis in an anti-Drebrin-seropositive patient. Exposure of primary hippocampal neurons to anti-Drebrin autoantibodies resulted in aberrant synapse composition and Drebrin distribution as well as increased spike rates and the emergence of burst discharges reflecting network hyperexcitability.
Interpretation: Anti-Drebrin autoantibodies define a chronic syndrome of recurrent seizures and neuropsychiatric impairment as well as inflammation of limbic and occasionally cortical structures. Immunosuppressant therapies should be considered in this disorder.

The notion that neuropsychiatric symptoms, including recurrent seizures and impairment of cognition and behavior, are linked to distinct autoantibodies (ABs) has fundamentally improved the diagnostic and therapeutic approaches for several severe neurological disorders.[1,2] This includes the disease spectrum of limbic encephalitis (LE).[3–6] Typically, cerebral magnetic resonance imaging (cMRI) reveals a swelling of the amygdala and other limbic structures, but MRI can also show discrete and non-specific abnormalities, or it can even be normal.[7] Neuropathological findings in corresponding brain biopsies range from predominantly lymphocyte-driven inflammation of limbic structures to the neuronal damage pattern of hippocampal sclerosis (HS).[8]

In LE, the AB spectrum comprises "onconeural" antibodies, including antibodies against amphiphysin (anti-AMPH), BMP-binding endothelial regulator (anti-BMPER, anti-CV2), paraneoplastic Ma antigen 2 (anti-Ma2, anti-PNMA2), and a key presynaptic protein, anti–glutamic acid decarboxylase 65 (anti-GAD65),[9] all of them aimed against intracellular protein structures. ABs targeting neuronal surface proteins suggest pathogenic concepts of hyperexcitability. These targets include N-methyl-D-aspartate receptors, leucine-rich glioma inactivated 1, contactin-associated protein 2, α-amino-3-hydroxy-5-methyl-4-isoxazolepropionic acid receptors (AMPARs), γ-aminobutyric acid receptor B, dipeptidyl-peptidase-like protein-6, metabotropic glutamate receptor 5, and glycine receptors.[1]

Despite the progress in recognizing AB-mediated immune mechanisms in a substantial proportion of patients with encephalitis and particularly LE, specific "neurological" ABs are not detected in a substantial fraction of patients with symptoms suspicious for LE.[3,10] This may partially be explained by a limited spectrum of ABs tested at individual centers and potentially restricted sensitivities of individual test systems. However, many encephalitis patients with unclear etiology remain without definite diagnosis even after extensive evaluation also for infectious etiologies.[11] A better understanding of immunological mechanisms in so-far seronegative encephalitis patients opens new therapy options for affected individuals.[12,13]

Here, we report on clinical and immunological characteristics of 4 patients who presented neuropsychiatric symptoms and seizures suggesting autoimmune encephalitis/LE and ABs against a so-far unrecognized antigen, Drebrin (**d**evelopmentally **r**egulated **br**ain prot**ein**).[14] Complementary in vitro analyses suggest that patient-derived anti-Drebrin ABs induce impaired synapse composition and neuronal hyperexcitability.

Patients and Methods

Patients

In 4 patients with neuropsychiatric symptoms including recurrent seizures and impairment of cognition and behavior, we observed a prominent band around 70kDa by immunoblotting after incubation with the patient sera, which was not present when blots were incubated with sera/cerebrospinal fluid (CSF) from healthy controls.

In none of the 4 patients were common "neurological" ABs detected using commercial kits for diagnostic procedures. All procedures were conducted in accordance with the Declaration of Helsinki. Informed written consent was obtained from every patient.

Neuroimaging

Patients underwent cMRI in 2 different systems. A 3-dimensional T1-weighted sequence was acquired on an Achieva 3.0T TX (Philips Healthcare, Best, the Netherlands) with the following parameters: voxel size = $1 \times 1 \times 1mm^3$, repetition time (TR) = 8.1 milliseconds, echo time (TE) = 3.7 milliseconds, flip angle = 8°, matrix = 256×256 pixels. A T1-weighted magnetization-prepared rapid acquisition gradient echo sequence was acquired on a 3T Siemens MAGNETOM Trio (Siemens Healthineers, Erlangen, Germany) using a 32-channel head coil (voxel size = $0.8 \times 0.8 \times 0.8mm^3$, TR = 1,660 milliseconds, TE = 2.54 milliseconds, flip angle = 9°, matrix = 320×320 pixels). Volumetric analysis of the amygdala, the hippocampus, and intracranial volume was carried out using the FreeSurfer v6.0.0 image analysis suite.[15,16] Parcellation results were visually checked for accuracy and alignment by 2 independent raters. All analyzed volumes were adjusted by the intracranial volume minus the ventricular volume.

Neuropathology

Biopsy brain tissue of one retrospectively anti-Drebrin AB[+] patient was neurosurgically removed for diagnostic purposes. As described before, tissue was fixed in paraformaldehyde (PFA) overnight and embedded in paraffin. Deparaffinized 4μm sections were stained with hematoxylin and eosin and commercial antibodies specific for cluster of differentiation 3, cluster of differentiation 8, neuronal nuclei, glial fibrillary acidic protein, and human leukocyte antigen–DR isotype. Staining was visualized using the avidin-biotin-peroxidase method.[17]

Control Cohort

Biomaterial of 31 healthy donors (male, n = 14; female, n = 17; mean age 33.6 ± 10.2 standard deviation) and from 85 patients with adult onset epilepsy and suspected LE showing reactivity in immunoblot screening (bands at 60–75kDa and/or 120–140kDa, as observed in the index patient) were used as controls and were obtained and analyzed exactly as the biomaterial of the anti-Drebrin AB[+] patients.

Screening Tests for Novel Autoantibodies

Screening tests for potential novel ABs comprise immunoblotting and indirect immunofluorescence test (IIFT). For immunoblots, protein lysates of rat and mouse brain, of human hippocampal tissue from pharmacoresistant temporal lobe epilepsy patients undergoing epilepsy surgery for seizure relief,[18] and of murine crude synaptosomes[19] were isolated, separated by electrophoresis, and blotted. After blocking with 2% (wt/vol) bovine serum albumin (BSA), 2% (wt/vol) fetal calf serum, 0.2% (wt/vol) cold water fish gelatin in phosphate-buffered saline (PBS), proteins were

incubated with serum (1:500) and CSF (1:100) overnight at 4°C, washed with PBS/Tween 20, incubated with goat anti-human IRDye 800CW (Odyssey, 926-32232; LI-COR, Lincoln, NE) for 45 minutes, and imaged with the Odyssey Imaging System (LI-COR) after another washing step.

For IIFT screening, a custom-made biochip-based-assay (Neurologie-Mosaik28; Euroimmun, Lübeck, Germany; FA 111-1005-28) was used including rat and Simiiformes slices of cerebellum and hippocampus to screen for binding patterns of ABs in sera and CSF of LE patients (dilution: serum, 1:10; CSF, 1:1). All IIFT assays were analyzed by an expert examiner (A.J.B.).

Immunoprecipitation and Mass Spectrometry

Immunoprecipitation (IP) was conducted as recently described.[20] Briefly, 1g of freshly dissected rat brain tissue was homogenized in 5ml buffer (100mmol/l Tris[hydroxy-methyl]-aminomethane–HCl, pH 6.5, 150mmol/l sodium chloride, 1 mmol/l ethylenediaminetetraacetic acid, 1% [wt/vol] sodium deoxycholate, 1% [wt/vol] Triton X-100, 1% [wt/vol] N-octyl-beta-D-glucopyranoside) containing protease inhibitors. Lysate was rotated 3 hours at 4°C and centrifuged at 21,000 × g for 15 minutes at 4°C. The clear supernatant was incubated with biomaterial for 3 hours at 4°C before adding Protein G Dynabeads (Thermo Fisher Scientific, Waltham, MA) and incubating overnight. Beads were washed 3 times using buffer as outlined above. Elution was performed at 70°C for 10 minutes using NuPAGE LDS sample buffer (Thermo Fisher Scientific) containing 25mmol/l dithiothreitol. Prior to 4 to 12% sodium dodecyl sulfate–polyacrylamide gel electrophoresis (SDS-PAGE; NuPAGE system, Thermo Fisher Scientific), carbamidomethylation was performed. Proteins were visualized with Roti-Blue Solution (Carl Roth, Karlsruhe, Germany). Additional bands compared to patterns observed with serum/CSF from healthy controls were excised from the gel, destained, and dehydrated with 50 and 100% wt/vol acetonitrile. Proteins were digested by 0.4μg trypsin at 37°C for 6 hours. To extract the peptides, 100μl aceto-nitrile with increasing concentration (50%, 100% wt/vol) was added and incubated for 5 minutes, and the supernatant was collected. Peptides were lyophilized and transferred to mass spectrometry (MS) for protein identification.

Cloning of Drebrin Fragments

The full-length human Drebrin cDNA sequence was divided into 6 fragments of similar length with 51bp overlap at both ends of the fragments. Fragments were amplified using the following primers: fragment 1 (M^1-G^{127}): forward 5′-GCGGAATTCGATGGCCGGCGTCAGCTTC-3′, reverse 5′-GATGCGGCCGCCTAACCCGCGTCTATGTCTTC CACG-3′; fragment 2 (G^{111}-R^{236}): forward 5′-GCG

GAATTCGATGGGTGTCGACGTGATCGTGAACGC C-3′, reverse 5′-GATGCGGCCGCCTACCTGTGCT CCTCGATCTGCTGC-3′; fragment 3 (E^{220}-T^{335}): forward 5′-GCGGAATTCGATGGAGCGCGAGCGGCGC TACC-3′, reverse 5′-GATGCGGCCGCCTACGTGG GGATGGGAGTGGGCG-3′; fragment 4 (G^{319}-T^{444}): forward 5′-GCGGAATTCGATGGGCAGCCACCTGG ACAGCC-3′, reverse 5′-GATGCGGCCGCCTACGTG GCGTCAGCTGTGGCAG-3′; fragment 5 (E^{428}-E^{552}): forward 5′-GCGGAATTCGATGGAGCAGGCTGTCC TGGCTGCT-3′, reverse 5′-GATGCGGCCGCCTAC TCCCCTTCCACTTCCTCTGGGTCACAG-3′; fragment 6 (L^{536}-D^{649}): forward 5′-GCGGAATTCGATGC TGCCTGAGCCGCCAGCCA-3′, reverse 5′-GATGC GGCCGCCTAATCACCACCCTCGAAGCCCTCC-3′. Drebrin fragments 1 to 6 were cloned into pETDuet1-T7-His-hDrebrin(wt) (Addgene plasmid # 40362)[21] by replacement of the full-length Drebrin via EcoRI/NotI restriction sites. Plasmids were verified by sequencing.

Validation of Anti-Drebrin Autoantibody Binding.

Recombinant human Drebrin protein and Drebrin fragments 1 to 6 were purified by Ni$^+$-affinity purification following the QIAGEN protocol. Therefore, a pETDuet1-T7-His-hDrebrin(wt) plasmid (Addgene plasmid # 40362)[21] and the newly generated pETDuet1-T7-His-Drebrin fragments 1 to 6 were transformed into competent BL21 *Escherichia coli* cells. Protein expression was induced by addition of 0.1mM isopropyl β-D-1 thiogalactopyranoside, and cells were lysed in lysis buffer (50mmol/l sodium phosphate, 300mmol/l sodium chloride, 5mmol/l imidazole, pH 8.0) by sonication. After centrifugation of the lysate, the supernatant was incubated for 1 hour with Ni$^+$-nitrilotriacetic acid (NTA)-agarose (QIAGEN, Hilden, Germany). Ni$^+$-NTA-agarose was washed with wash buffer containing increasing imidazole concentrations (5–80mmol/l imidazole, 50mmol/l sodium phosphate, 300mmol/l sodium chloride, pH 8.0). The protein was eluted with 250mmol/l imidazole solution overnight.

Eight-hundred nanograms of the protein was loaded for SDS-PAGE and either stained with Coomassie[22] or blotted and blocked as described above. The membrane was transferred to a Mini-PROTEAN II Multiscreen Apparatus (Bio-Rad Laboratories, Hercules, CA) and incubated with different biomaterial (all 4 anti-Drebrin AB$^+$ patients, 31 healthy controls, and 85 LE patient controls; dilution: serum, 1:100; CSF, 1:1), commercial anti-Drebrin (ab12350; Abcam, Cambridge, MA; 1:1,000), and anti-His tag (ab18184, Abcam, 1:1,000) antibodies in blocking buffer overnight. Bands were visualized as described above using goat antimouse and goat antihuman IRDye 800CW (Odyssey, 926-32210, 926-32232) secondary antibodies.

Primary Hippocampal Neurons

Dissociated primary hippocampal neurons (PHNs) of embryonic day 15 (E15) to E19 murine hippocampi (C57Bl6/N) were prepared as described before[23] and cultured in NeuroBasal medium.

Quantification of Synapses and Immunohistochemistry

PHNs were fixed with 4% PFA in PBS for 10 minutes, followed by 3 PBS washing steps. Cells were permeabilized with PBS/Triton X-100 (0.3% [wt/vol]) for 10 minutes and blocked for 1 hour at room temperature (RT) with buffer containing 1% BSA and 10% normal goat serum (NGS). Neurons were incubated overnight with primary antibodies (anti-Drebrin, ab12350, Abcam, 1:1,000; anti–postsynaptic density protein 95 (PSD95), 75-028, NeuroMab, Davis, CA, 1:500; anti-Homer, 160004, Synaptic Systems, Göttingen, Germany, 1:1,000) or sera (1:100) of respective patients in PBS/Triton X-100 (0.1% [wt/vol]) in blocking buffer at 4°C. After 3 PBS washing steps, Alexa Fluor secondary antibodies (goat antihuman A11013, Invitrogen; goat antimouse A11001, Invitrogen 1:1,000; goat anti–guinea pig A11-073, Invitrogen 1:1,000) and 4,6-diamidino-2-phenylindole (DAPI; 1:100) in PBS/Triton X-100 were incubated for 45 minutes in blocking buffer. Before mounting with Mowiol, cells were washed 3 times.

To quantify the colocalization of anti-Drebrin ABs with the key excitatory postsynaptic scaffolding proteins Homer1 and PSD95, 3 biological replicates consisting of 3 technical replicates each were imaged with a laser-scanning Nikon (Tokyo, Japan) A1/Ti confocal microscope with a Plan APO IR 60× WI objective (NA 1.27). Imaging conditions were kept constant for all conditions. Data were processed with Nikon NIS-Elements 4.0 acquisition software, and colocalization of the antibody with patient anti-Drebrin was quantified using ImageJ software (Fiji).

Anti-Drebrin Antibody Uptake Assay

For the binding assay, cells were incubated at in vitro day 14 (DIV14) for 48 hours with either commercial anti-Drebrin antibody (ab12350, Abcam; 20μg/ml, 10μg/ml, 2μg/ml, 1μg/ml) or corresponding concentrations of human control IgG (Intratect; Orifarm, Odense, Denmark). Cells were washed with PBS and immediately fixed with PFA in PBS at DIV16 for 10 minutes, followed by 3 washing steps. Neurons were permeabilized with PBS/Triton X-100 (0.3% [wt/vol]) for 10 minutes, blocked in buffer containing PBS/Triton X-100 (0.1% [wt/vol]) with 1% BSA and 10% NGS for 1 hour at RT, and incubated overnight with Alexa Fluor secondary antibodies (goat antihuman A11013, Invitrogen; goat antimouse A11001, Invitrogen; 1:1,000) and DAPI (1:100). The next day, cells were washed 3 times and mounted with Mowiol. Images were taken with a laser-scanning Nikon A1/Ti confocal microscope.

Functional Analysis of Human Anti-Drebrin Autoanti-bodies

For functional analyses, IgG fraction from Patient 1 serum was purified via Protein G HP Ab Spin Trap Kit (GE Healthcare, Chicago, IL; 28-4083-47) according to the manufacturer's protocol. PHNs on coverslips were incubated at DIV14 for 20 minutes or 48 hours either with affinity-purified anti-Drebrin patient IgG fraction or with control IgG. After incubation, cells were washed, fixed, permeabilized, and blocked as described above. After incubation with primary (anti-Drebrin, ab12350, Abcam, 1:1,000; anti-Homer, 160004, Synaptic Systems, 1:1,000) and appropriate secondary antibodies, cells were washed and mounted. Images were taken with a laser-scanning Nikon A1/Ti confocal microscope.

For each condition, 3 biological and 6 technical replicates captured in 5 stacks (0.3μm steps) were analyzed. Synapses were identified by using Homer1 staining and analyzed by generating the maximum intensity projection (ImageJ). Intensity was set as a 20% threshold from the maximum intensity of the Homer1 staining. Synapse size was set between 0.02 and 0.4 μm^2.

Recording and Analysis of Network Activity in Hippocampal Neurons

Multielectrode arrays (MEAs) simultaneously recorded signals from 16 electrodes per well from neurons grown on CytoView-MEA-24-well-plates with a sampling frequency of 12.5 kHz (Maestro Edge; Axion Biosystems, Atlanta, GA). Spikes were detected by an adaptive threshold defined as 6.5 × standard deviation, whereas bursts were defined by using an interspike interval (ISI) threshold with a maximum of 100 milliseconds and a minimum number of 5 spikes within a burst recorded by a single electrode. Network bursts were defined as a collection of at least 50 spikes across an entire well (not limited to one electrode) with an ISI of 100 milliseconds. In addition, a minimum number of 6 active electrodes must contribute to a network burst. in vitro neuronal network activity (ivNNA) was measured with pooled anti-Drebrin AB+ sera from all 4 patients diluted 1:100 starting on DIV14 compared to normal human serum (NHS) and to native cultures. Data were recorded at different time points after starting the incubation (10 minutes, 30 minutes, 60 minutes, and 4 hours) and recorded with AxIS software (Axion Integrated Studio Navigator 1.5., Axion Biosystems).

Immunohistochemistry with Wild-Type and Drebrin Knockout Mice

Adult male Drebrin knockout[24] and age-matched wild-type mice were sacrificed under deep isoflurane anesthesia. Brains were quickly removed and fixed in 4% PFA for 1 hour at 4°C, incubated in 40% sucrose for another 24 hours, and snap frozen in isopentane chilled with liquid nitrogene.[13] Eighteen-micrometer-thick cryosections were air-dried and sequentially incubated with 3% H_2O_2 and 0.5% Triton X-100 for 20 minutes, 10% NGS for 1 hour, and patient or control serum (1:100) or a monoclonal mouse anti-Drebrin antibody (ab12350, Abcam, 1:1,000) at 4°C overnight. After using the appropriate secondary biotinylated antibodies (Life Technologies, Carlsbad, CA; 1:500), the reactivity was examined by the standard avidin-biotin-peroxidase method.[25]

Statistical Analysis

Experiments were conducted in a randomized and blinded fashion. Statistical analyses were performed with GraphPad (San Diego, CA) Prism 6.05 software. Sample size (n) per experiment was calculated using power analysis, with parameters set within the accuracy of the individual experiment. Values were considered significantly at $p < 0.05$. All results are plotted as mean ± standard error of the mean.

Results

All 4 patients who tested positively for anti-Drebrin AB (anti-Drebrin AB[+]; 1 male, 3 females; age at onset = 45 years, range = 23–68) developed a subacute progressive encephalopathy with major symptoms of neuropsychiatric impairment involving depression and cognitive impairment and/or confirmed or clinically suspected focal epileptic seizures or status epilepticus (Tables 1 and 2). CSF alterations comprised increased protein levels in all patients as well as mononuclear cell pleocytosis in at least one individual. cMRI alterations in T2-weighted images included dynamic hippocampal volume changes as well as extrahippocampal atrophy (representative cMRI imaging of Patient 2 in Fig 1A–D). In 3 patients (Patients 1–3), individual immunotherapies were positively correlated with seizure control, AB titer decrease, and/or neuropsychological performance. However, given the limited number of data points, the specificity of these correlations may be limited (see Fig 1E–H, Table 2). Cerebral brain tissue for neuropathological analysis was available for one of these cases (Patient 4) gained from a diagnostic brain biopsy 10 years after disease onset, which revealed a chronic T-lymphocytic–driven encephalitis with attack of neurons (see Fig 1I–N). The index patient (Patient 1) presented a neuropil binding pattern on rodent and Simiiformes hippocampal slices in the serum sample (data not shown). Immunoblot analysis with sera of the index patient revealed several bands, including the most prominent band at ~70kDa, in brain homogenates from human, rat, and mouse as well as in synaptosome lysate (Fig 2A, asterisk) that were absent in blots incubated with control sera (data not shown). This observation suggested the presence of ABs other than common neurological ABs, which had been ruled out previously, in this serum sample.

Identification of the Target Antigen Drebrin

Following the IP of rat brain lysate with antibodies isolated from the serum of the index patient (Patient 1), a Coomassie-stained SDS-PAGE also showed an additional 70kDa band (see Fig 2B, asterisk), which was not present in any of the controls (3 epileptic and 2 healthy controls). MS of this band identified Drebrin (molecular weight = 71kDa) as the most abundant protein present in the sample in multiple independent experiments. The detection of multiple bands in the immunoblot screening of brain and synaptosome homogenates in the present patient series is putatively due to protein degradation, complex post-translational modification of Drebrin, or unspecific binding of other antibodies present in the serum. This assumption is supported by our observation that immunoblotting with sera from healthy controls also resulted in the detection of background immunoreactivity. However, it can also not entirely be ruled out that the ABs, characterized as targeting Drebrin here, bind with lower affinity also to unrelated proteins, although we did not find immediate evidence for this scenario in the present test battery.

To establish a screening assay, we purified polyhistidine-(6x-His)-tagged recombinant human Drebrin protein from bacteria for immunoblotting experiments with patient sera (see Fig 2C). Immunoblotting with the serum of the index patient (Patient 1) showed a band at the expected size of ~130kDa. Drebrin has been reported to run higher than its calculated mass in SDS-PAGE due to strong negative charge of the protein.[26,27] Next, we screened the serum of all 4 patients—Patient 1 and 3 patients with equivalent results in the initial immunoblot screening of brain and synaptosome homogenates—as well as a mouse monoclonal anti-Drebrin antibody, as positive control. For all 4 patient sera tested, we observed reactivity at ~130kDa (see Fig 2D). In addition, the serum of all 4 patients showed a punctate labeling pattern on permeabilized cultured mouse PHNs reflecting the pattern of the mouse monoclonal anti-Drebrin antibody (representative immunohistochemistry [IHC] in Fig 2E).

The anti-Drebrin AB titer in the 4 patients' sera ranged from 1:1,000 to 1:10,000; in 3 patients, anti-Drebrin ABs were also detected in corresponding CSF samples, with

TABLE 1. Clinicoserological Parameters of Anti-Drebrin Autoantibody-Positive Patients

Pat.	Age at Seizure Onset, yr	Sex	Binding Pattern	HEp2	CSF	EEG	Additional Diagnosis	Symptoms	Time Point (mth/y)	MRI
#1	50	M	Neuropil	neg	↑ Protein levels	Slowing L temp	CGL (FD: 2017), asthma medication: fluticasone furoate/ vilanterol	Memory impairment, status epilepticus	07/16	Swelling hip bilateral
									01/17	↓ V hip R
									07/17	Swelling hip R
#2	38	F	—	ANA	↑ Protein levels	Focus R temp	Episodes of night sweats (FD: 2015)	Unaware focal seizures	05/15	Swelling hip + amy R constant
									08/15	Constant
									04/16	Constant
#3	68	F	Neuropil	neg	↑ Protein levels	Focus L temp	Polymyalgia rheumatica (FD: 2012), medication: MTX, Pred.	Unaware focal seizures; bradycardia	06/15	Swelling amy L
									11/16	Constant
#4	23	F	—	neg	↑ Protein levels, pleoc.	Focus L temp	Selective IgA deficiency, numbness and paresis of R hand, R visual field loss	Unaware focal/ bilateral tonic-clonic seizures; epilepsia partialis continua	07/02	Normal
									08/06	Gliosis hem L
									09/12	Gliosis hem L
									08/13	Constant
									08/16	Progressive
									02/17	Constant
									08/17	Constant
									01/18	Constant

Swelling refers to volume increase and T2/fluid-attenuated inversion recovery hyperintensity.

↑ = increase; ↓ = decrease; amy = amygdala; ANA = antinuclear antibodies; CGL = chronic granulocytic leukemia; CSF = cerebrospinal fluid; EEG = electroencephalography; F = female; FD = first diagnosis; hem = hemisphere; hip = hippocampus; L = left; M = male; MRI = magnet resonance imaging; MTX = methotrexate; neg. = negative; Pat. = Patient; pleoc. = pleocytosis; Pred. = prednisolone; R = right; temp = temporal; V = volume; Time point (mth/y) = time point of consultation.

a titer ranging from 1:1 to 1:100. Positive IIFT results were observed in sera of patients (Patients 1 and 3) with particularly high abundance of anti-Drebrin ABs. Evaluation of possible intrathecal synthesis of IgG based on Reiber's formula[28] suggested intrathecal IgG synthesis in Patient 2 with a relative CSF/sera LSQ_{rel} (Limes quotient) value of 11.75 (<1.5 = positive). There is evidence of intrathecal synthesis of specific antibodies if the CSF/serum quotient of specific antibodies (LSQ_{spec}) is significantly higher than the CSF/serum quotient of total IgG (LSQ_{ges}). The relationship between these two values is called the relative CSF–serum ratio LSQ_{rel}. For Patient 1 (LSQ_{rel} = 0.05) and Patient 4 (LSQ_{rel} = 0.38), no evidence of intrathecal synthesis was present at the time of analysis, and for Patient 3, sufficient clinical data were not available.

Sera from both control groups consisting of 31 healthy donors or 85 patients with chronic epilepsy with similar findings in immunoblot screenings (bands at 60–75kDa and/or 120–140kDa) did not show any reactivity to the recombinant Drebrin protein (data not shown).

TABLE 2. Neuropsychological Dynamics Correlated with Clinicoserological Parameters of Anti-Drebrin AB+ Patients

Pat.	Time Point	AED[a]	IS	MRI	AB Status[b]	IQ	Exec. Mem.	Verb. Mem.	Fig. Mem.	BDI
#1	07/16	Val (1,200)		R hip ↑	1:5,000 (S) 1:1 (CSF)	+++	++++	+++	0	+++
	01/17	Lam (250)		R hip ↓	Negative		++++	++	0	+++
	07/18	Lam (400)		R hip ↑	Negative	+++	++++	+++	0	+++
#2	08/15	Lev (1,500)		R amy ↑	1:2,500 (S) 1:100 (CSF)	+++	+++	++++	+++	+++
	03/16	Lam (400)		R amy ↑	1:2,500 (S)		+++	++++	+++	+++
	03/17	Lam (400)				+++	++	++++	+++	+++
#3	06/15	Lev (2,000)	Pred. p. + Pred. (2.5)	L amy ↑ (09/15)	1:10,000 (S) Negative (CSF)	+++	+++	+++	+++	+++
	12/15	Lev (2,000)	Pred. (2.5)	L amy ↑			+++	+++	+++	+++
	11/16	Lev (3,000), Lac (200)	Pred. (2.5)		Negative (S) Negative (CSF)		+++	++	+	+++
#4	02/13	Lev (3,000), Oxc (300)		L hemis ↓ (06/13)	1:5,000 (s[c]) 1:10 (csf[c])	+++	0	0	+	
	07/16	Lev (4,000)	Pred. p.	L par ↑, temp-pol ↑	1:1,000 (S) Negative (CSF)	+++	0	+	+	+++
	02/17	Lev (4,000), Clob (50), Zon (600)	Pred. p.	L hemis ↓			0	+	+	+++
	08/17	Lev (4,000)	Pred. p.	No further dynamic			+	+++	+	+++
	04/19	Lev (4,000), Clob (50), Zon (600)		L hemis ↓			0	+++	+++	+++

Empty spaces indicate no data available for these time points.

[a]Numbers refer to daily dosage in milligrams.

[b]Anti-Drebrin AB status; numbers refer to specific titers.

[a](06/13).

+ = performance = 2 SD below average; ++ = performance = 1 SD below average; +++ = average performance; ++++ = performance above average; ↑ = volume increase; ↓ = volume decrease; AB = autoantibody; AED = antiepileptic drug; amy = amygdala; 0 = performance > 2 SD below average; BDI = Beck Depression Inventory; Clob = clobazam; CSF = cerebrospinal fluid; Exec. = executive; Fig. = figural; hemis = hemisphere; hip = hippocampus; IQ = intelligence quotient; IS = immunosuppressant therapy; L = left; Lac = lacosamide; Lam = lamotrigine; Lev = levetiracetam; Mem. = memory; MRI = magnet resonance imaging; Oxc = oxcarbazepine; p. = pulse; par = parietal; Pat. = Patient; Pred. = prednisolone; R = right; S = serum; SD = standard deviation; temp-pol = temporopolar; Val = valproate; Verb. = verbal; Zon = zonisamide.

Characterization of Anti-Drebrin Autoantibody Binding Regions

To investigate in detail which region of Drebrin is bound by the patient-derived ABs, we divided the Drebrin protein coding sequence into 6 overlapping fragments (see Fig 2F), which were purified of bacteria and analyzed by SDS-PAGE. Due to their high content of negative charge, the size of Drebrin fragments 1, 4, 5, and 6 as revealed by
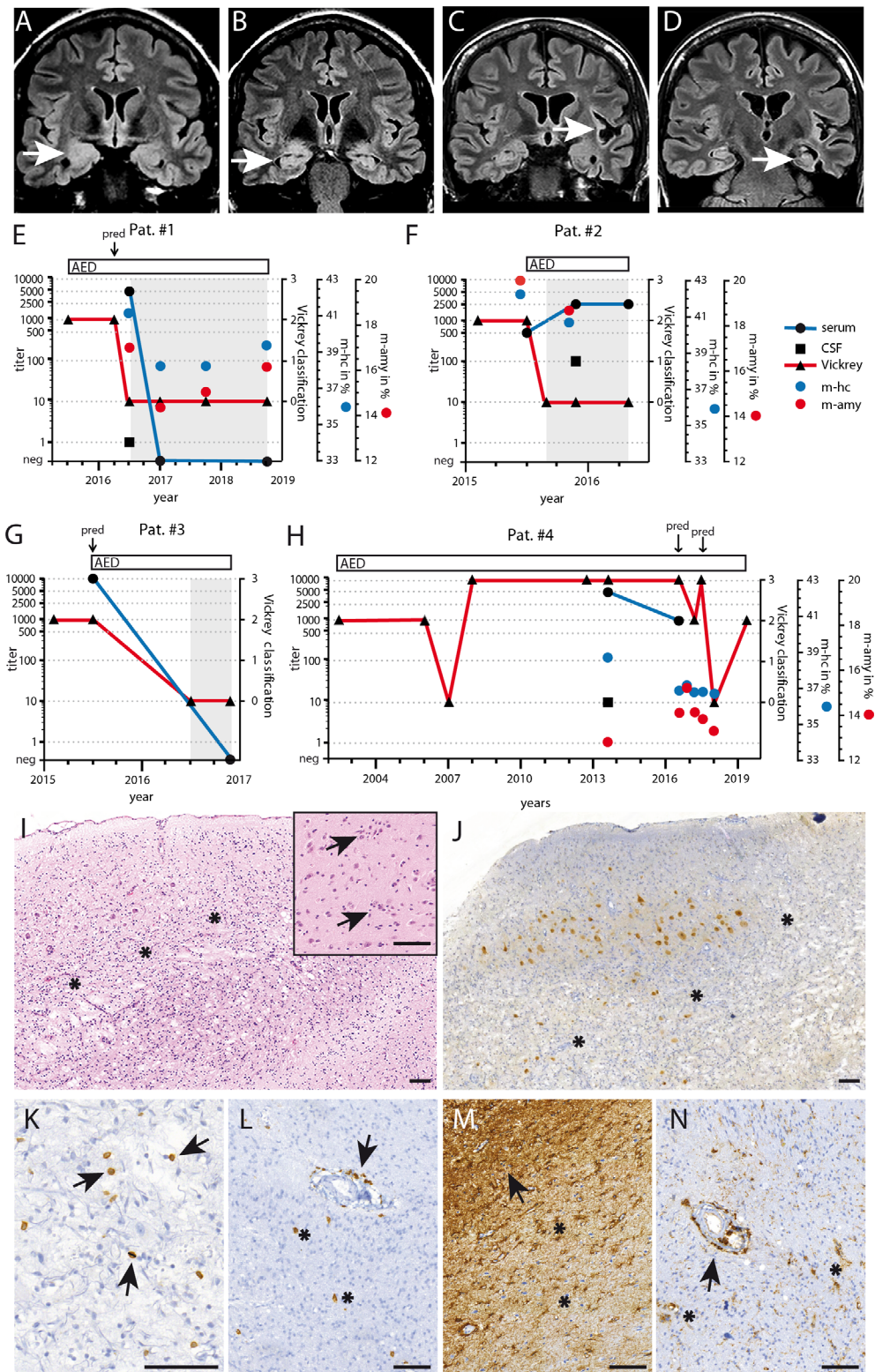
FIGURE 1: Representative cerebral magnetic resonance imaging (cMRI), clinical aspects, and neuropathological findings in anti-Drebrin autoantibody-positive patients. (A–D) Findings on cMRI scans (T2–fluid-attenuated inversion recovery images) ranged from very subtle to extensive changes involving not only limbic but cortical structures. cMRI of Patient 2 revealed (A) swelling and T2-hyperintensity of the right amygdaloid area (*white arrow*) as well as (B) a certain loss of the internal organoid texture of the right-sided hippocampal formation (*white arrow*). (C) In contrast to these circumscribed limbic changes, in Patient 4 the cMRI showed extensive atrophy of the left hemisphere (*white arrow*) as well as some swelling of the left amygdala. (D) Additionally, there was only a slight volume reduction of the left hippocampus (*white arrow*). (E–H) Clinical aspects. In Patients 1, 3, and *(Figure legend continues on next page.)*

Coomassie staining of the SDS-PAGE differed from the calculated one,[26,27] similar to full-length Drebrin (see Fig 2C). Immunoblots with serum of Patient 2 showed a strong immunoreactivity with Drebrin fragment 6 and a weaker binding to fragment 4. The same fragments were also detected by the other 3 patient sera. Fragment 4 was bound by ABs from sera of Patients 3 and 4; fragment 6 was detected by ABs in serum of Patient 1. Fragments 1–3 and 5 did not show a reaction with any patient's sera (see Fig 2G).

Anti-Drebrin Autoantibody Revealed a Strong Colocalization with Dendritic Structures

Next, we examined the binding pattern of anti-Drebrin ABs from patients on PHNs. We observed a pronounced immunolabeling toward the neuropil, especially at dendritic spines, which looked similar to the one obtained with a commercial monoclonal anti-Drebrin antibody (representative IHCs shown in Fig 3A). All patients' anti-Drebrin ABs showed a colocalization with the key excitatory postsynaptic scaffolding proteins PSD95 and Homer1 (representative stainings shown in Fig 3B). Quantification of synaptic structures positive for sera from 4 anti-Drebrin AB[+] patients revealed colocalization in >90% of synapses with Drebrin (commercial antibody), Homer1, and PSD95 (see Fig 3).

Anti-Drebrin Antibodies Are Taken Up into Neurons

To probe whether patient-derived anti-Drebrin ABs target intracellular structures, cultured PHNs were incubated with various concentrations of commercial anti-Drebrin antibodies at 37°C for 48 hours to allow antibody uptake. After extensive washing, neurons were permeabilized and antihuman secondary antibodies were added. Only incubation with 20μg/ml antibody, not various lower concentrations, resulted in a specific dendritic binding pattern (see Fig 3F, left; representative staining in Fig 3F, right).

No labeling was also observed after incubation with different concentrations of control IgG. Therefore, anti-Drebrin antibodies can be taken up by PHNs. However, detection of internalized anti-Drebrin antibody requires high antibody concentrations; this prohibits the visualization of anti-Drebrin ABs from patient sera due to the relatively low titers in sera/CSF.

Incubation of Hippocampal Neurons with Anti-Drebrin ABs Alters Postsynaptic Drebrin Levels and Distribution as Well as Neuronal Excitability

To analyze a potential impact of patient-derived anti-Drebrin AB incubation on postsynaptic Drebrin abundance and localization, primary hippocampal cultures were incubated for either 20 minutes or 48 hours at 37°C with affinity-purified IgG from serum of Patient 1 or control IgG. Postsynapses were identified by labeling with anti-Homer1 antibodies (see Fig 3G; region of interest [ROI]). Drebrin abundance and synaptic distribution were analyzed by quantifying the intensity and size of the commercial anti-Drebrin immunosignal within the anti-Homer1–defined ROIs (see Fig 3G, left). Incubation with purified IgG from patients with anti-Drebrin ABs caused an increase in the size as well as the fluorescence intensity of the anti-Drebrin fluorescent signal compared to incubation with control IgG (see Fig 3G, right), indicating an accumulation of Drebrin protein in synaptic structures as a potential pathogenic effect.

To test for acute functional consequences of patient-derived anti-Drebrin AB on ivNNA of primary hippocampal cultures, their activity was measured using MEAs. ivNNA reflects intrinsic network properties in the absence of extrahippocampal sensory inputs and allows for exclusively testing patient anti-Drebrin AB effects on hippocampal network activity.

Spontaneous network activity was recorded 10 minutes, 30 minutes, 1 hour, and 4 hours after incubation with anti-Drebrin AB[+] patient sera and compared with that obtained from NHS incubation or age-matched

---

4, improvement in seizure control correlated with immunotherapy. Amygdala and hippocampal volume parameters assessed by serial cMRI scans in Patients 1 and 4 revealed a reduction when patients were under immunotherapy. Patient 2 improved clinically on antiepileptic drugs (AEDs). Seizure-free intervals are highlighted in gray. Outcome (*triangles*) is reported based on Vickrey's classification: 0, seizure-free; 1, aura; 2, 1–10 seizures/yr; 3, >10 seizures/yr. Amygdala/hippocampal volume (isometric T1-sequence) is given as mean relative volume of both amygdalae/hippocampi (m-amy/m-hc) as a percentage. CSF = cerebrospinal fluid; Pat. = Patient; pred = prednisolone pulse. (I–N) Neuropathological findings in a cortical biopsy of Patient 4 show rather dense mononuclear infiltrates in hematoxylin & eosin stain that became visible with a focus in deeper cortical layers (I, *asterisks*). There was substantial edema and also lymphocytes clustering around neurons (I, *black arrows* in *insert*); macrophage infiltrates were also present. (J) Immunohistochemistry with antibodies against NeuN demonstrated substantial neuronal cell loss in the lower cortical layers (*asterisks*). (K) Mononuclear infiltrates corresponded to CD3-positive T-lymphocytes (*black arrows*) as well as (L) CD8-positive T-lymphocytes clustered around blood vessel structures (*arrow*) and in intraparenchymal localization (*asterisks*). (M) Concomitantly, extensive fibrillary (*black arrow*) and cellular astrogliosis (*asterisks*) was present in the glial fibrillary acidic protein immunohistochemistry. (N) Correspondingly, immunohistochemistry with antibodies against human leukocyte antigen–DR isotype demonstrated abundance of activated, highly ramified microglial infiltrates (*asterisks*) as well as the presence of macrophages, some of them with perivascular localization (*black arrow*; all scale bars correspond to 100μm). No syndecan-positive plasma cells were present (data not shown). [Color figure can be viewed at www.annalsofneurology.org]
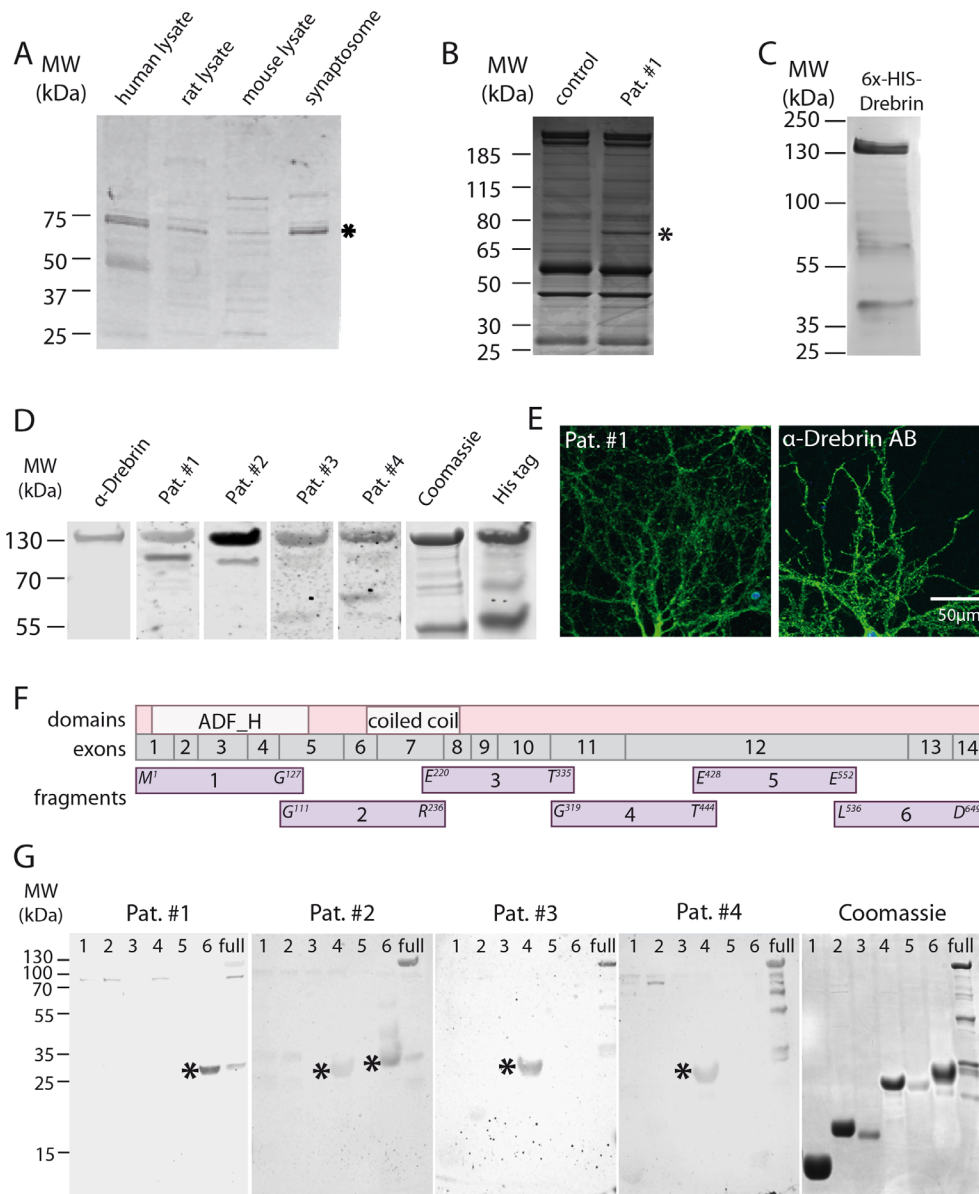
FIGURE 2: Identification of a novel autoantibody as anti-Drebrin and target epitope mapping. (A) Immunoblotting of human, rat, mouse, and synaptosome homogenates with representative patient's serum revealed a strong immunoreactive signal ~70kDa (*asterisk*). (B) Coomassie-stained sodium dodecyl sulfate–polyacrylamide gel electrophoresis (SDS-PAGE) after immunoprecipitation performed with serum of an immunoblot screening negative control and index patient (Patient 1) showed a strong signal at ~70kDa (*asterisk*), which was only present in the patient sample and was identified by mass spectrometry as Drebrin. (C) Coomassie labeling of human Drebrin protein purified from bacteria. Due to the large number of negatively charged residues in the protein, the detected band size differs from the calculated molecular weight. (D) Sera of the 4 patients included in the present series showed reactivity against the purified human Drebrin protein (shown in the Coomassie-stained SDS-PAGE), as did an antibody against the His-tag present in the purified protein. (E) Representative immunolabeling of human anti-Drebrin autoantibodies (ABs) from index Patient 1 in cultured primary hippocampal neurons compared to a mouse monoclonal anti-Drebrin antibody. Both showed a similar neuropil expression pattern with strong immunoreactivity on dendritic spines, supporting a binding to the same target protein Drebrin. (F) Depiction of the full-length Drebrin protein, showing its domains, exon structure, and the overlapping Drebrin fragments 1 to 6 assessed as targets of AB binding. (G) Representative immunoblots of the full-length Drebrin and its fragments 1 to 6 labeled with human ABs from sera of Patients 1 to 4 detected full-length Drebrin and fragments 4 and/or 6 (*asterisks*). Coomassie staining shows the amount of purified proteins loaded for immunoblotting. MW = molecular weight; Pat. = Patient. [Color figure can be viewed at www.annalsofneurology.org]

native cultures (representative MEA traces shown in Fig 4A). We observed a temporally altered activity pattern after patient-derived anti-Drebrin AB⁺ sera incubation, which was able to synchronize neuronal activity and led to bursts with substantially prolonged duration (see Fig 4B).

Anti-Drebrin AB⁺ patient sera already strongly increased the activity of hippocampal neurons after
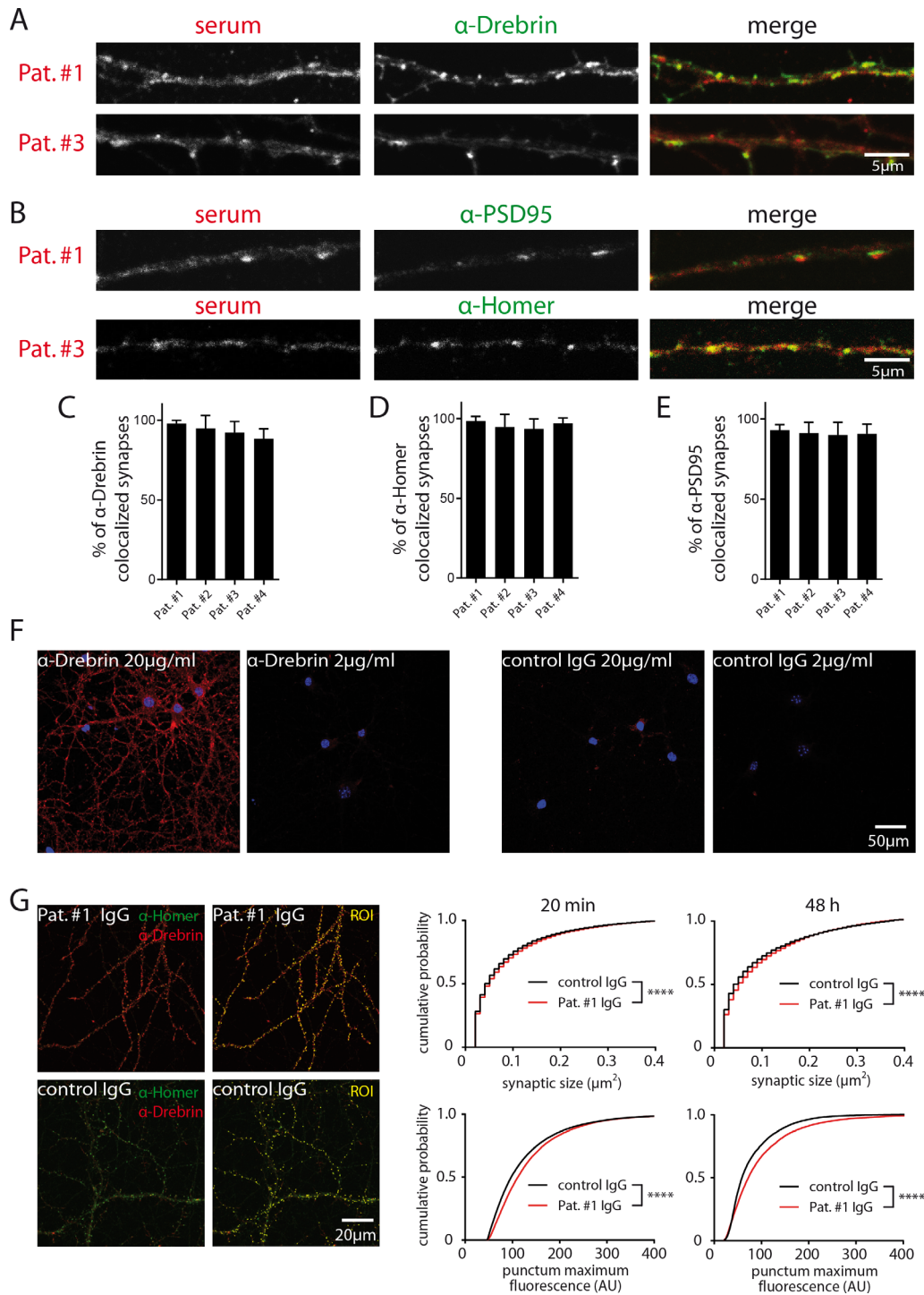
FIGURE 3: Uptake of human anti-Drebrin autoantibody (AB) alters postsynaptic Drebrin abundance and distribution. (A) Anti-Drebrin AB[+] patients' sera and monoclonal mouse anti-Drebrin antibody strongly labeled dendritic spines, in which Drebrin is enriched. (B) Costaining with antibodies against postsynaptic proteins PSD95 as well as Homer showed a strong colocalization at dendritic spines, indicating the presence of Drebrin at excitatory postsynapses. (C–E) A similar degree of colabeling was observed for sera from all anti-Drebrin AB[+] patients with (C) Drebrin (D) Homer or (E) PSD95. (F) Representative staining of primary hippocampal neurons incubated with commercial anti-Drebrin antibody or control IgG using different concentrations. Incubation for 48 hours at 37°C with high concentrations of anti-Drebrin antibody or control IgG (left; 20μg/ml) on in vitro day 14 or with lower concentrations (right; 2μg/ml) revealed intracellular uptake of the anti-Drebrin at high antibody concentrations. Counterstain with DAPI was used (blue). (G) Representative image of primary hippocampal neurons incubated either with purified IgG fraction from Patient 1 or control IgG for synapse morphology analysis. Incubation with purified IgG fraction from Patient 1 led to increased synaptic size and synaptic fluorescence intensity after 20 minutes as well as after 48 hours (Kolmogorov–Smirnov test: ****$p < 0.0001$ for both parameters and time points). Pat. = Patient; ROI = region of interest. [Color figure can be viewed at www.annalsofneurology.org]
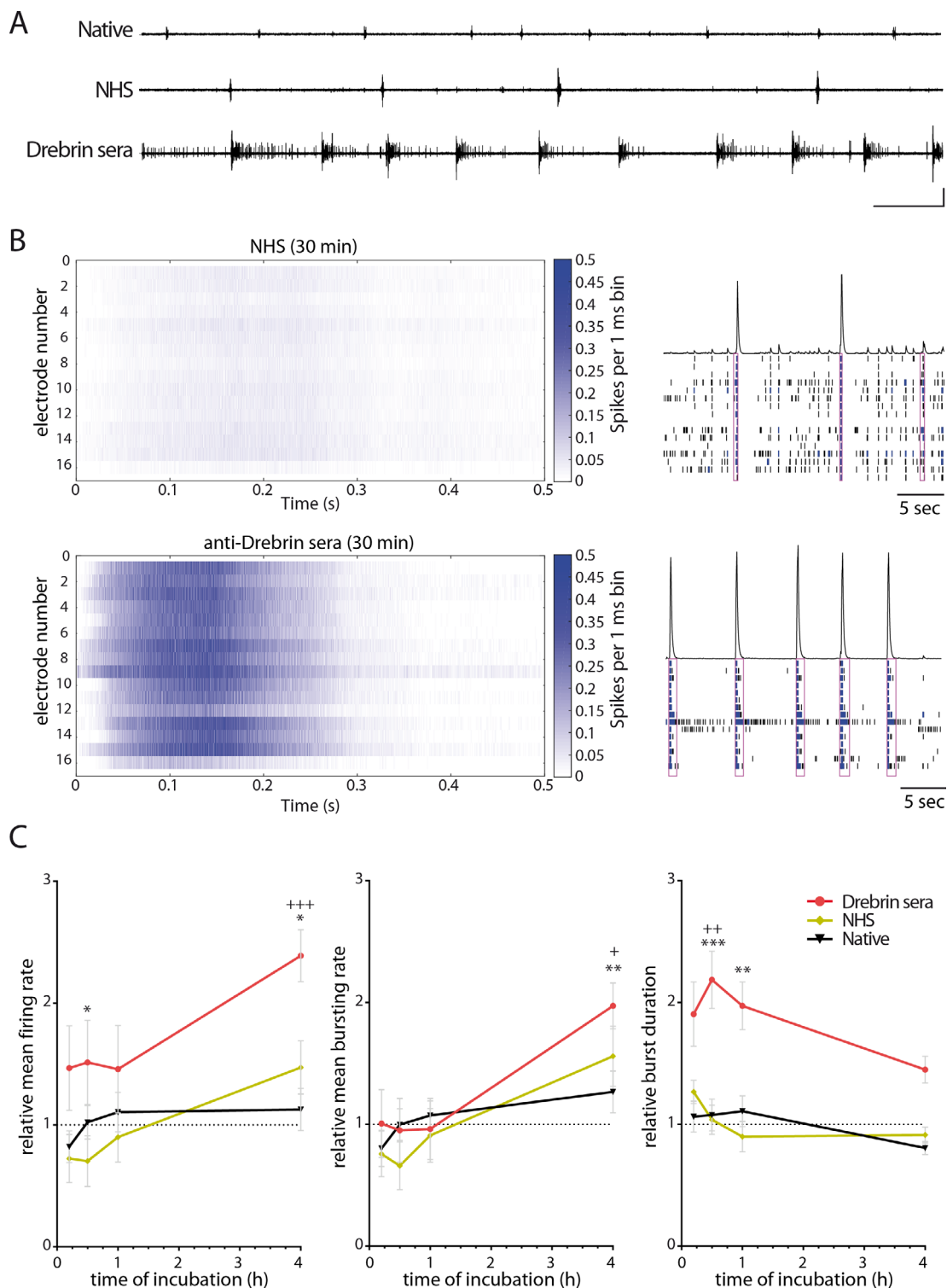
FIGURE 4: Increased neuronal network activity in cultured hippocampal neurons. (A) Anti-Drebrin autoantibody (AB)[+] sera led to increased neuronal activity compared to normal human serum (NHS) and native neurons recorded with multielectrode arrays (MEAs; representative traces of spontaneous neuronal activity; vertical scale bar = 25μV; horizontal scale bar = 5 seconds). (B) Spiking and bursting activity is shown for neurons incubated with NHS and for neurons treated with anti-Drebrin AB[+] sera. The spike time histograms (left) display an average contribution of all 16 electrodes per well to an average network burst during the whole recording of 20 minutes. Note the reproducibility of the temporal activity patterns occurring within and between electrodes of the anti-Drebrin AB[+] sera-treated well. The representative raster plots show timing of spikes in a 30-second recording period (right). Magenta rectangles indicate the duration of the network burst. (C) Incubation with anti-Drebrin AB[+] sera led to increased network activity. The mean firing (left) and bursting rates (center) were analyzed in naive mouse cultures (n = 3 MEAs), in cultures incubated with NHS, or in anti-Drebrin AB[+] sera (n = 3 MEAs each; incubation at *(Figure legend continues on next page.)*

30 minutes of application, whereas NHS incubation was without an effect (see Fig 4C). The impact of patient-derived anti-Drebrin AB⁺ sera was persistent and progressive. After 4 hours, the mean firing rate and the bursting rate were significantly increased compared to corresponding values of NHS-incubated control neurons. These data suggest that anti-Drebrin ABs acutely elevate network activity by increasing synaptic connectivity and synaptic excitability of neurons. Interestingly, the burst duration, demonstrating a higher and longer-lasting activity of neurons, displayed an early increase after incubation with patient anti-Drebrin AB⁺ sera.

Validation of Anti-Drebrin Autoantibodies in Drebrin Knockout Mice

To finally verify the presence of anti-Drebrin ABs in the patients' biomaterial, we used brain slices from Drebrin knockout and age-matched wild-type mice and exposed them to anti-Drebrin AB⁺ patients' sera. The sera of all 4 patients, as well as the commercial anti-Drebrin antibody showed strong reactivity on wild-type mouse slices, with an increased binding in the hippocampal formation and the cerebellar molecular layer (Fig 5). This pattern was completely absent in the tissue of knockout mice and within the negative control.

Discussion

Here, we report on 4 patients with a novel autoimmune syndrome, which is characterized by the presence of anti-Drebrin ABs, focal epilepsy onset in adulthood, and variable degrees of cognitive and behavioral impairment. Additionally, patients had a swelling and T2-signal increase of the amygdala and hippocampi, followed by HS as well as atrophic changes of extrahippocampal limbic and extratemporal brain structures. Unilateral predilection of MRI changes in AB-related encephalitis is not unusual, as it has been reported to occur for example in anti–GAD65 AB⁺ patients.[12] The novel AB target Drebrin is a key component of neurites and excitatory synaptic structures with intracellular postsynaptic localization. Support for an autoimmune etiology of this syndrome is further provided by elevated protein levels in the CSF of 3 patients as well as the presence of accompanying systemic rheumatic symptoms or immune cell neoplasms.

Starting from the AB in sera/CSF of the patients, 5 sets of experiments indicated Drebrin as the AB target. Those were (1) IP of Drebrin from brain/synaptosome protein lysate with AB present in patients' sera; (2) the detection of identical band patterns in immunoblots with a commercial anti-Drebrin antibody as with the patients' sera; (3) corresponding binding patterns in PHNs of a commercial anti-Drebrin antibody with the patients' sera compared to controls, indicating an accumulation of the AB target in dendritic spines; (4) identification of 2 Drebrin protein domains, which serve as epitopes for AB recognition; and (5) comparative immunohistochemical analysis of wild-type and Drebrin knockout mice, showing no immunoreactivity with patients' sera in the brains of Drebrin knockout mice. Furthermore, our in vitro data point to a direct pathogenetic effect of the patient-derived anti-Drebrin AB, as they bind to postsynaptic Drebrin, impair postsynaptic Drebrin abundance and distribution, and induce neuronal network hyperexcitability.

The clinical courses and neuroradiological and neuropathological data of anti-Drebrin AB⁺ patients indicated that this disease condition is severe. Individual patients had to be hospitalized several times, and the spectrum of major clinical symptoms comprises cognitive impairment as well as focal epileptic seizure activity. The symptom onset in adulthood throughout all patients, the occurrence of relapses, and the clinical responses to immunotherapy even after prolonged disease duration are well in line with immune-mediated disease mechanisms in these 4 anti-Drebrin AB⁺ patients. Intriguingly, brain biopsy tissue was available from one patient with extensive unilateral temporal and extratemporal atrophy (see Fig 1). Although the admixture of neuronal degeneration accompanied by predominant cytotoxic T-lymphocytic and activated microglia infiltrates was considered to be compatible with Rasmussen encephalitis, nodular microglial architectures were not striking. The neuropathological pattern, however,

---

in vitro day 14 after baseline recording). The increase in neuronal activity was temporarily enhanced in anti-Drebrin AB⁺ sera-incubated cultures with respect to spike firing rate at 30 minutes (*p = 0.033 Drebrin vs NHS) and 4 hours after incubation (+++p = 0.0004 Drebrin vs native, *p = 0.013 Drebrin vs NHS) as well as for the bursting rate 4 hours after application (+p = 0.0215 Drebrin vs native, **p = 0.0014 Drebrin vs NHS). The duration of spontaneous bursts of anti-Drebrin AB⁺ incubated neurons was increased early after incubation compared to NHS and to native cultures (30 minutes: ***p = 0.0007 Drebrin vs NHS, ++p = 0.0054 Drebrin vs native, 1 hour: **p = 0.0013 Drebrin vs NHS). Firing rate, 2-way analysis of variance (ANOVA): interaction, p = 0.226, $F_{8, 135}$ = 1.346; group comparison, ****p < 0.0001, $F_{2, 135}$ = 11.01; time comparison, **p = 0.0019, $F_{2, 135}$ = 4.519; Tukey post hoc test. Bursting rate, 2-way ANOVA: interaction, p = 0.48, $F_{8, 135}$ = 0.947; group comparison, ****p < 0.0001, $F_{2, 135}$ = 11.55; time comparison, ****p < 0.0001, $F_{4, 135}$ = 7.125; Tukey post hoc test. Burst duration, 2-way ANOVA: interaction, *p = 0.01, $F_{8, 135}$ = 2.629; group comparison, ***p = 0.0002, $F_{2, 135}$ = 8.977; time comparison, ***p < 0.005, $F_{4, 135}$ = 5.39; Tukey post hoc test. Data are normalized to the averaged baseline recording of each condition. Plus signs indicate Drebrin versus Native; asterisks indicate Drebrin versus NHS. [Color figure can be viewed at www.annalsofneurology.org]
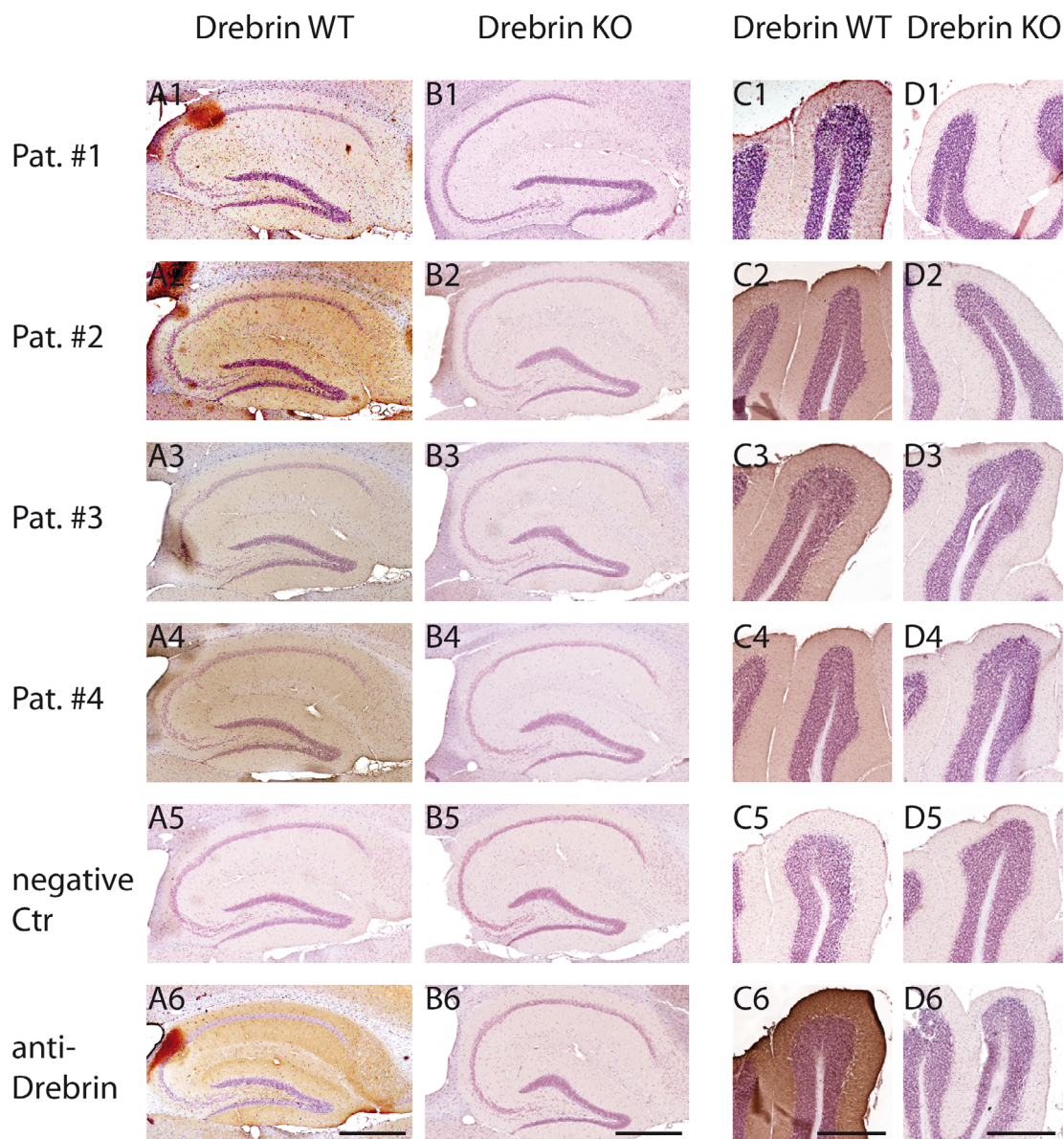
FIGURE 5: Comparison of individual patients' sera reactivity using brain slices from Drebrin knockout versus wild-type (WT) mice. (A_{1-4}) Anti-Drebrin autoantibody (AB)$^+$ patient sera and (A_6) a mouse monoclonal anti-Drebrin antibody showed a strong labeling within the hippocampal formation in WT mice. (B_{1-4}) In contrast, no binding pattern was detectable on hippocampal slices in a parallel experiment using hippocampi from Drebrin knockout mice. (B_6) Staining was also absent with the commercial mouse monoclonal anti-Drebrin antibody. (C_{1-4}) Correspondingly, the present binding pattern in the cerebellar molecular layer in WT mice (D_{1-4}) was abrogated in the Drebrin knockout mice (C_6, D_6), similar to the mouse monoclonal anti-Drebrin antibody. No staining was visible in the negative control (Ctr) using normal human serum (A_5, B_5, C_5, D_5). Note the delicate neuropil binding pattern in the hippocampi and the cerebellar molecular layer of WT mice incubated with anti-Drebrin AB$^+$ patients' sera, strongly recapitulating the pattern of mouse monoclonal anti-Drebrin antibody (scale bars = 500μm for all). Pat. = Patient. [Color figure can be viewed at www.annalsofneurology.org]

largely reflects findings in affected brain structures of anti-GAD65 AB$^+$ patients.[12] Likewise, the considerable discrepancy between progressive brain tissue destruction, variable seizure dynamics, and neuropsychological aspects, even involving transient improvement, are rather similar to clinical observations in anti-GAD65 AB$^+$ patients.[29] However, the presence of anti-GAD65 ABs was ruled out in the present patient series.

Furthermore, the notion of Drebrin as a molecule with intracellular localization as well as the neuropathological admixture of neurodegeneration with invasion of T-lymphocytes in the biopsy tissue of Patient 4 may suggest analogies of the present disease pattern with other paraneoplastic neurological syndromes. In this context, experimental data for anti-Pnma1 AB-related encephalitis suggest pathogenetically critical T-lymphocytes target identical

molecular structures as the corresponding onconeuronal AB.[30] Antiamphiphysin ABs induce presynaptic vesicle dynamic impairment[31] in parallel to T-cell–mediated damage.[32] For anti-Drebrin ABs, our present in vitro data point to functional impairment of synaptic structures and network hyperexcitability. The exact contribution of anti-Drebrin ABs versus T-lymphocyte inflammatory components to the pathology in patients will require intense studies in the future.

The hyperexcitability observed in cultured hippocampal neuronal networks treated with patient-derived anti-Drebrin ABs is in line with increased excitability of affected brain structures emerging as seizures in seropositive patients. Our electrophysiological in vitro data are consistent with the view that anti-Drebrin ABs act on the level of synapses (higher frequency of network bursts). Furthermore, as the effect of anti-Drebrin ABs occurred very soon after incubation (∼10–30 minutes), we propose that their effect does not require a transcriptional or translational response. Rather, it appears likely that anti-Drebrin ABs act directly via binding their target. Antibodies cannot readily penetrate cell membranes themselves, and it is therefore not directly evident how anti-Drebrin ABs could reach their intracellular target. However, synaptic activity, such as that spontaneously generated by cultured hippocampal neurons, permanently goes along with endocytotic processes regulating for example the number of postsynaptic AMPARs in synapses. We suggest that anti-Drebrin ABs use such endocytosis cycles as an entry route to the intracellular compartment. Ultimately, antibody-bound Drebrin may well disturb spine function and lead to a pathological synaptic uncoupling, which can then be seen as neuronal network hyperexcitability. Future, combined molecular and super-resolution studies are needed to assess this important aspect of the pathophysiological sequelae of anti-Drebrin ABs.

Drebrin loss is observed in postmortem brains of individuals with mild cognitive impairment[33] and Alzheimer disease (AD)[34,35] as well as in animal models of AD.[36,37] However, pronounced seizure activity has so far not been reported in Drebrin knockout mice. This may be because compensatory mechanisms can evolve, particularly in the context of the constitutive ablation of Drebrin. Interestingly, after pilocarpine-induced status epilepticus the expression of Drebrin A is transiently reduced in affected hippocampi, particularly during epileptogenesis,[38] which has been functionally related to impaired dendritic actin cytoskeleton dynamics and synaptic dysfunction.

An intriguing implication of this study is the possibility of immunosuppressant therapy as an option for patients with suspected encephalitis manifesting with neuropsychological impairment and/or seizure activity and with anti-Drebrin ABs. Although the frequency of this disorder is currently still unresolved, we expect further cases to be detected by regular serological testing of patients suspicious for (limbic) encephalitis.

Acknowledgment

Author Contributions

J.P., J.C.K., D.D., S.S., C.E.E., and A.J.B. contributed to the conception and design of the study; J.P., D.K., A.B., J.C.K., D.D., T.R., G.L., R.v.W., C.H., H.V., R.S., and A.J.B. contributed to the acquisition and analysis of data; J.P., D.K., A.B., J.C.K., E.H., S.S., and A.J.B. contributed to drafting the text and preparing the figures. P.E.G. contributed to the acquisition and analysis of data.

Potential Conflicts of Interest

A patent is pending for the use of anti-Drebrin ABs for diagnostic purposes (Euroimmun, S.S./A.J.B./University of Bonn). The other authors have nothing to report.

References

1. Leypoldt F, Armangue T, Dalmau J. Autoimmune encephalopathies. Ann N Y Acad Sci 2015;1338:94–114.

2. Vincent A, Bien CG, Irani SR, Waters P. Autoantibodies associated with diseases of the CNS: new developments and future challenges. Lancet Neurol 2011;10:759–772.

3. Soeder BM, Gleissner U, Urbach H, et al. Causes, presentation and outcome of lesional adult onset mediotemporal lobe epilepsy. J Neurol Neurosurg Psychiatry 2009;80:894–899.

4. Irani SR, Bien CG, Lang B. Autoimmune epilepsies. Curr Opin Neurol 2011;24:146–153.

5. Irani SR, Michell AW, Lang B, et al. Faciobrachial dystonic seizures precede Lgi1 antibody limbic encephalitis. Ann Neurol 2011;69: 892–900.

6. Saiz A, Blanco Y, Sabater L, et al. Spectrum of neurological syndromes associated with glutamic acid decarboxylase antibodies: diagnostic clues for this association. Brain 2008;131:2553–2563.

7. Heine J, Pruss H, Bartsch T, et al. Imaging of autoimmune encephalitis—relevance for clinical practice and hippocampal function. Neuroscience 2015;309:68–83.

8. Bauer J, Bien CG. Neuropathology of autoimmune encephalitides. Handb Clin Neurol 2016;133:107–120.

9. Graus F, Delattre JY, Antoine JC, et al. Recommended diagnostic criteria for paraneoplastic neurological syndromes. J Neurol Neurosurg Psychiatry 2004;75:1135–1140.

10. Brenner T, Sills GJ, Hart Y, et al. Prevalence of neurologic autoantibodies in cohorts of patients with new and established epilepsy. Epilepsia 2013;54:1028–1035.

11. Gable MS, Gavali S, Radner A, et al. Anti-NMDA receptor encephalitis: report of ten cases and comparison with viral encephalitis. Eur J Clin Microbiol Infect Dis 2009;28:1421–1429.

12. Malter MP, Helmstaedter C, Urbach H, et al. Antibodies to glutamic acid decarboxylase define a form of limbic encephalitis. Ann Neurol 2010;67:470–478.

13. Boronat A, Gelfand JM, Gresa-Arribas N, et al. Encephalitis and antibodies to dipeptidyl-peptidase-like protein-6, a subunit of Kv4.2 potassium channels. Ann Neurol 2013;73:120–128.

14. Shirao T, Obata K. Two acidic proteins associated with brain development in chick embryo. J Neurochem 1985;44:1210–1216.

15. Fischl B, Salat DH, Busa E, et al. Whole brain segmentation: automated labeling of neuroanatomical structures in the human brain. Neuron 2002;33:341–355.

16. Fischl B, Salat DH, van der Kouwe AJ, et al. Sequence-independent segmentation of magnetic resonance images. Neuroimage 2004;23: S69–S84.

17. Alvarez-Baron E, Bien CG, Schramm J, et al. Autoantibodies to Munc18, cerebral plasma cells and B-lymphocytes in Rasmussen encephalitis. Epilepsy Res 2008;80:93–97.

18. Blumcke I, Spreafico R, Haaker G, et al. Histopathological findings in brain tissue obtained during epilepsy surgery. N Engl J Med 2017; 377:1648–1656.

19. Evans GJ. Subcellular fractionation of the brain: preparation of synaptosomes and synaptic vesicles. Cold Spring Harb Protoc 2015; 2015:462–466.

20. Scharf M, Miske R, Kade S, et al. A spectrum of neural autoantigens, newly identified by histo-immunoprecipitation, mass spectrometry, and recombinant cell-based indirect immunofluorescence. Front Immunol 2018;9:1447.

21. Geraldo S, Khanzada UK, Parsons M, et al. Targeting of the F-actin-binding protein Drebrin by the microtubule plus-tip protein EB3 is required for neuritogenesis. Nat Cell Biol 2008;10:1181–1189.

22. Laemmli UK. Cleavage of structural proteins during the assembly of the head of bacteriophage T4. Nature 1970;227:680–685.

23. van Loo KMJ, Rummel CK, Pitsch J, et al. Calcium channel subunit α2δ4 is regulated by early growth response 1 and facilitates epileptogenesis. J Neurosci 2019;39:3175–3187.

24. Jung G, Kim EJ, Cicvaric A, et al. Drebrin depletion alters neurotransmitter receptor levels in protein complexes, dendritic spine morphogenesis and memory-related synaptic plasticity in the mouse hippocampus. J Neurochem 2015;134:327–339.

25. Pitsch J, Schoch S, Gueler N, et al. Functional role of mGluR1 and mGluR4 in pilocarpine-induced temporal lobe epilepsy. Neurobiol Dis 2007;26:623–633.

26. Kreis P, Hendricusdottir R, Kay L, et al. Phosphorylation of the actin binding protein Drebrin at S647 is regulated by neuronal activity and PTEN. PLoS One 2013;8:e71957.

27. Shirao T, Hanamura K, Koganezawa N, et al. The role of Drebrin in neurons. J Neurochem 2017;141:819–834.

28. Reiber H. External quality assessment in clinical neurochemistry: survey of analysis for cerebrospinal fluid (CSF) proteins based on CSF/serum quotients. Clin Chem 1995;41:256–263.

29. Hansen N, Widman G, Witt JA, et al. Seizure control and cognitive improvement via immunotherapy in late onset epilepsy patients with paraneoplastic versus GAD65 autoantibody-associated limbic encephalitis. Epilepsy Behav 2016;65:18–24.

30. Pellkofer H, Schubart AS, Hoftberger R, et al. Modelling paraneoplastic CNS disease: T-cells specific for the onconeuronal antigen PNMA1 mediate autoimmune encephalomyelitis in the rat. Brain 2004;127:1822–1830.

31. Werner C, Pauli M, Doose S, et al. Human autoantibodies to amphiphysin induce defective presynaptic vesicle dynamics and composition. Brain 2016;139:365–379.

32. Poh MQ, Simon NG, Buckland ME, et al. Evidence of T-cell mediated neuronal injury in stiff-person syndrome with anti-amphiphysin antibodies. J Neurol Sci 2014;337:235–237.

33. Counts SE, Nadeem M, Lad SP, et al. Differential expression of synaptic proteins in the frontal and temporal cortex of elderly subjects with mild cognitive impairment. J Neuropathol Exp Neurol 2006;65: 592–601.

34. Shim KS, Lubec G. Drebrin, a dendritic spine protein, is manifold decreased in brains of patients with Alzheimer's disease and Down syndrome. Neurosci Lett 2002;324:209–212.

35. Counts SE, He B, Nadeem M, et al. Hippocampal Drebrin loss in mild cognitive impairment. Neurodegener Dis 2012;10:216–219.

36. Lacor PN, Buniel MC, Furlow PW, et al. Abeta oligomer-induced aberrations in synapse composition, shape, and density provide a molecular basis for loss of connectivity in Alzheimer's disease. J Neurosci 2007;27:796–807.

37. Mahadomrongkul V, Huerta PT, Shirao T, Aoki C. Stability of the distribution of spines containing Drebrin A in the sensory cortex layer I of mice expressing mutated APP and PS1 genes. Brain Res 2005; 1064:66–74.

38. Ferhat L. Potential role of Drebrin A, an F-actin binding protein, in reactive synaptic plasticity after pilocarpine-induced seizures: functional implications in epilepsy. Int J Cell Biol 2012;2012:474351.